APST

Asia-Pacific Journal of Science and Technology

Investigation of the metallurgical microstructure resulting from underwater welding at depths of 3 and 5 meters using UW-1 and E6013 welding electrodes.

Arawan Chanpahol[1], Saksirichai Srisawat[1], Boonsin Nadondu[1], Thongchai Khrueaphue[1,*] and Parinyawatr Dhinnabutra[2]

[1]Program in Industrial Engineering Technology and Logistics, Faculty of Agricultural and Industrial Technology, Phetchabun Rajabhat University, Thailand 67000
[2]Program of Welding Engineering, Faculty of Technical Education, Rajamangala University of Technology Isan, Khon Kaen, Thailand 40000
*Corresponding author: Thongchai.k@pcru.ac.th

Abstract

This study presents a comparative analysis of underwater welding using E6013 and UW-1 electrodes on carbon steel at depths of three and five meters. The investigation focuses on weld quality, microstructure, and hydrogen content. At a depth of three meters, both electrodes produced welds that met standard criteria and were free of porosity, slag inclusion, and cracking. UW-1 produced smoother and more completely fused surfaces, aided by the forehand welding technique and proper electrode angle, which promoted stable metal transfer and clear visibility of the molten pool. scanning electron microscope (SEM) analysis revealed alternating martensite and pearlite in the weld zone (WZ), with E6013 producing more martensite and a coarser structure in the heat-affected zone (HAZ), along with visible separation from the base metal. Energy Dispersive X-ray Spectroscopy technology (EDS) analysis showed hydrogen content in the WZ was 11.02% for E6013 and 6.50% for UW-1, the latter being lower than typical underwater welding levels (7.0–11.7%). In the HAZ, E6013 and UW-1 showed 5.23% and 5.06% hydrogen, respectively. The results suggest that E6013 can serve as a temporary substitute for UW-1 in shallow underwater welding, but its use should be limited to depths not exceeding three meters due to quality control constraints at greater depths.

Keywords: Underwater welding, Hydrogen, Carbon steel, UW-1 electrode, E6013 electrode

1. Introduction

　　Thailand is now making significant and ongoing efforts to expand and enhance its maritime industry. Thailand possesses a significant advantage due to its dual-coast marine sector, which covers both the Gulf of Thailand and the Andaman Sea. These areas serve as major centers for the production and transportation of local and international commodities, including the oil drilling industry and maritime freight transportation. The majority of materials utilized in these industries are metallic, which are susceptible to fracture due to prolonged usage, deterioration, and corrosion caused by contact with seawater. Therefore, it is imperative to perform maintenance in order to prolong the lifespan of such components or machinery. Industries such as these possess substantial components, such as oil drilling platforms and sizable cargo ships, which present challenges in terms of mobility and require significant expenses for each lifting procedure during onshore maintenance. As a result, repairs are often not financially beneficial when carried out on land, which is why underwater maintenance is preferred.

　　The wet underwater welding method necessitates individuals with exceptional proficiency in both diving and welding. This method is dependent on multiple stringent elements that have an impact on both safety and the quality of work. Presently, underwater maintenance is extensively employed for the reparation of offshore oil rig foundations and the hulls of sizable cargo vessels, whereby components are submerged at depths ranging from around three to 30 meters [1]. Frequent exposure to seawater leads to corrosion of these parts, resulting in changes
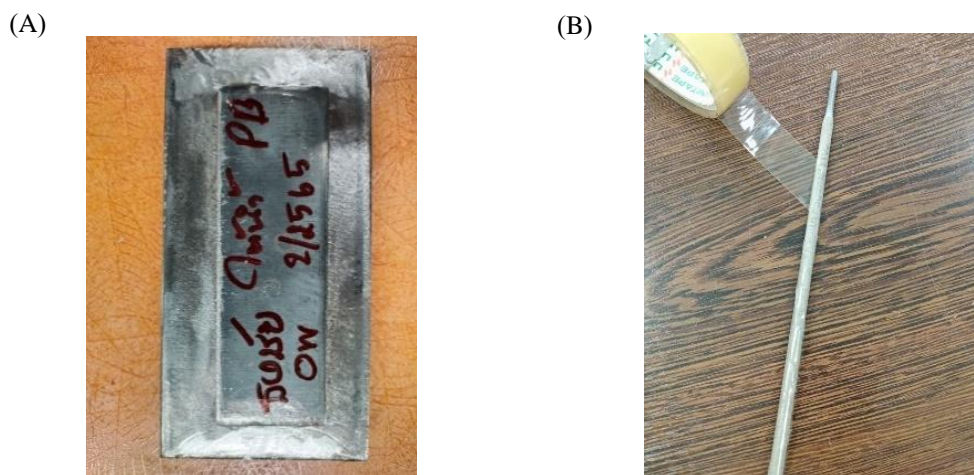
to their material properties and makes them more susceptible to damage. Furthermore, cracks in a ship's hull may occur due to collisions with rocks or the effect of sea waves. Similar forces can also damage the foundation of offshore drilling platforms, leading to fractures from seawater corrosion. Likewise, sections of certain dam types also experience deterioration. Failure to perform maintenance can result in futher damage.

Nevertheless, research has indicated that existing underwater welding electrodes are costly and have limited availability in the marketplace. Hence, the objective of this study is to assess the viability of replacing UW-1 underwater welding rods with AWS E6013 land welding rods [3] in order to lower welding expenses. The reason for this is that E6013 welding electrodes are more cost-effective and readily available compared to UW-1 welding rods, and both varieties exhibit similar chemical properties. In addition, the metallurgical properties of welds arising from water pressure and the amount of hydrogen in the water during welding are compared by studying the welding process at depths of three and five meters [1,3]. In underwater welding, hydrogen from the surrounding water environment can easily diffuse into the weld metal, which leads to critical issues, such as hydrogen-induced cracking and porosity [4,5]. These defects significantly compromise the mechanical strength of the weld. This phenomenon is difficult to avoid due to the nature of the underwater environment. However, it is possible to reduce the hydrogen diffusion rate by adjusting the electrode angle and employing appropriate welding techniques [6]. The novelty of this study lies in the experimental application of an alternative welding technique involving a tilted electrode angle of ten–15 degrees (compared to the typical 75–85 degrees used in dry welding), a forehand welding method, and a rear-view approach during operation—whereas conventional dry welding generally uses the backhand technique. This integrated method has rarely been studied systematically in underwater conditions [7]. The key advantages of this technique include enhancing the stability of electrode melting, minimizing hydrogen accumulation in the weld area, and improving slag control under water pressure. Once the welding process is complete, the surface of the weld, together with its macrostructure and microstructure, is analyzed using a scanning electron microscope (SEM). This inspection involves analyzing the elements and composition of the weld using Energy Dispersive X-ray Spectroscopy technology (EDS).

2. Materials and Methods

2.1 Preparation of Materials for Experimentation

This study investigates the application of wet underwater repair welding utilizing carbon steel materials of AH36 grade. A base plate measuring 200 x 100 x 9 millimeters and two assembly plates measuring 160 x 60 x 9 millimeters were fabricated and subsequently connected using a double lap joint technique, as depicted in Figure 1(A). This technique is frequently employed for the maintenance and restoration of ships [8,9]. Subsequently, E6013 welding electrodes with a diameter of 4 mm were prepared. A practical modification was applied by wrapping a transparent adhesive tape around the electrode core to prevent water from penetrating and mixing with the flux coating. The tape was overlapped by one-third of its width and wrapped from the tip to the end of the electrode in a single turn, as illustrated in Figure 2(B). This method was selected due to the availability of materials, low cost, good resistance to water ingress, and its simplicity compared to other coating techniques. In this study, the welding process was repeated three times. The chemical compositions of carbon steel, the E6013 electrode, and the underwater welding electrode UW-1 are shown in Table 1. [10,11]

(A)   (B)

Figure 1 Prepare the test material for underwater welding. (A) Carbon steel material and (B) welding electrode E6013.

Table 1 Presents the chemical composition of carbon steel and welding electrode, expressed in terms of weight.

AWS class	C (%)	Si (%)	Mn (%)	P (%)	S (%)	Cu (%)	Ni (%)
Carbon steel (AH36)	≤ 0.18	0.10-0.50	0.90-1.60	≤ 0.035	≤ 0.035	≤ 0.35	≤ 0.40
UW-1	~ 0.1	~ 0.43	~ 0.5	~ 0.015	~ 0.008	-	-
E6013	0.08-0.09	0.28-0.64	0.39-1.15	0.01-0.04	0.08-0.01	-	-

2.2 Procedure for Underwater Welding

Underwater wet welding systems rely on the welding techniques of each diver, in addition to the proficiency of their diving skills [3,9,12]. The reason for this is that underwater welding is markedly distinct from welding performed on land. Underwater welding is characterized by significantly reduced visibility, which is contingent upon the quality of the water. The visibility of the weld pool is affected by the refraction of light and welding radiation, even when the water is clear. As a result, it is difficult to visually monitor the weld pool when welding [12,13]. Consequently, researchers have modified the technique for observing the weld pool, shifting it from the front to the back of the welding rod. This modification enables a more distinct perception of the liquefied metal reservoir as it effectively blocks the welding light and radiation from directly affecting our vision (a customized method) and propelling it in the forward direction (usually, welding is carried out in the backward direction on land). The procedure for tool preparation and welding steps is as follows:

Step 1: The welding experiment was conducted using a 600-ampere capacity welding machine, operated under a Direct Current Electrode Negative (DCEN) polarity. The welding current was set at 250 amperes, a value determined through preliminary calculations to ensure that the molten pool temperature exceeded the melting point of the base metal, as detailed below.

The heat input and thermal behavior at the weld pool during underwater welding were evaluated to understand the temperature distribution and potential thermal losses. The total heat input was estimated using the standard energy input equation for arc welding, as shown in Equation (1):

$$Q_{total} = \eta \times V \times I \times t \tag{1}$$

Where Q_{total} is the total heat input (J), η is the arc efficiency (assumed to be 0.7 for SMAW, V is the arc voltage (25 V), I is the welding current (250 A), and t is the arc time, assumed to be 50 seconds [14]. The resulting total heat input is:

$$Q_{total} = 0.7 \times 25 \times 250 \times 50 = 218{,}750 \text{ J}$$

In underwater conditions, a considerable portion of the heat is lost due to convective and conductive heat transfer to the surrounding water [15]., the assumed thermal losses were approximately 50% at a depth of three and 60% at five meters. Therefore, the effective heat input (Q_{eff}) is calculated by:

$$Q_{eff} = Q_{total} \times (1 \text{ - Loss Fraction}) \tag{2}$$

Substituting the values:

3-meter depth: $Q_{eff@3m} = 218{,}750 \times 0.5 = 109{,}375$ J

5-meter depth: $Q_{eff@5m} = 218{,}750 \times 0.4 = 87{,}500$ J

To estimate the maximum possible temperature in the molten pool, a simplified cylindrical weld pool model was adopted. Assuming a pool diameter of 6 mm and depth of 3 mm, the volume was calculated as:

$$V = \pi \times r^2 \times h = \pi \times (0.003)^2 \times 0.003 = 8.48 \times 10^{-8} \text{ m}^3$$

Given the density of AH36 steel ($\rho = 7{,}850$ kg/m³), the mass of the molten region was determined:

$$m = \rho \times V = 7{,}850 \times 8.48 \times 10^{-8} = 0.000665 \text{ kg}$$

The maximum weld pool temperature was estimated using the specific heat equation, assuming all effective heat contributes to raising the temperature of the molten metal:

$$T_{max} = Q_{eff} / (m \times c) + T_{initial} \tag{3}$$

Where c = 470 J/kg·°C is the specific heat of steel, and $T_{initial}$ = 25°C. Substituting values yield:

3-meter depth: $T_{3m, E6013}$ = 109,375 / (0.000665 × 470) + 25 = 2,095.7°C

5-meter depth: $T_{5m, E6013}$ = 87,500 / (0.000665 × 470) + 25 = 1,950.6°C

For the UW-1 electrode, which is designed specifically for underwater welding applications, the effective heat input was assumed to be 5% greater than that of the conventional E6013 electrode [16]. Thus, the estimated maximum pool temperatures were adjusted accordingly:

$T_{3m, UW1}$ = 2,095.7 × 1.05 = 2,200.5°C

$T_{5m, UW1}$ = 1,950.6 × 1.05 = 2,048.1°C

The results indicate that although thermal losses in underwater conditions are significant, the residual heat input is sufficient to generate molten pool temperatures exceeding the melting point of AH36 steel (~1,490°C), ensuring effective fusion in underwater shielded metal arc welding (SMAW) at both evaluated depths.

(A)   (B)

Figure 2 depicts an experiment on underwater welding conducted at a depth of three meters: (A) the underwater welding device is designed to operate at a depth of three meters, and (B) the underwater welding performed via scuba diving.
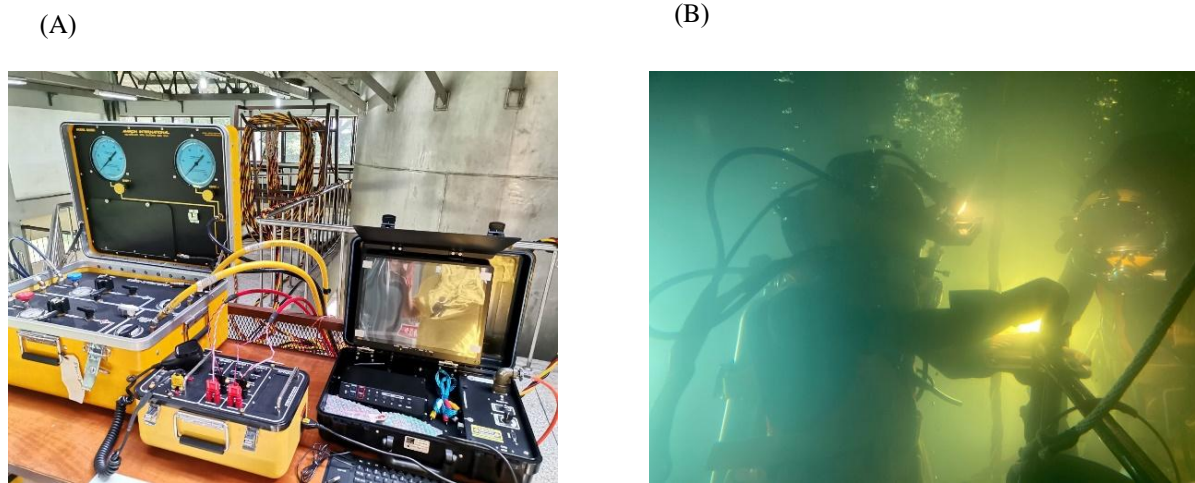
Step 2: Fill tanks with water to depths of three meters (Figure 2(A)) and five meters (Figure 2(B)). The experiment will take place at a vocational training institution in Songkhla Province, which is a part of the Department of Skill Development in Region 12.

Step 3: Prepare the scuba diving respiratory apparatus for welding at a depth of three meters. Place the workpieces in position and perform underwater welding on them (as shown in Figure 2(B)). Having backup divers available during welding is crucial for emergency assistance.

Step 4: Ready the subaquatic control apparatus (depicted in Figure 3(A)) to regulate welding operations at a depth of five meters. During underwater welding activities, a worker on land will oversee the operations while the welder uses a Kirby Morgan surface-supplied system to dive and weld (Figure 3(B)).

Step 5: Prior to analysis, ensure that the workpieces are properly prepared and examine the weld surface, macrostructure, and microstructure using a SEM that is equipped with EDS to accurately assess the elements and compositions present.

(A)

(B)

Figure 3 depicts an experiment on underwater welding conducted at a depth of five meters: (A) air diving activities conducted with surface-supplied equipment and (B) Underwater welding performed utilizing a Kirby Morgan surface-supplied system.

3. Results and Discussion

3.1 The Examination of the Weld Surface

According to the observations from Table 2, visual inspection of the underwater weld surface was performed in accordance with ANSI/AWS D3.6M:2017, Class C. The results show that welds produced using both E6013 and UW-1 electrodes met the acceptance criteria, exhibiting no porosity, no slag inclusions, and no visible cracks. However, welds performed using the E6013 electrode at both three- and five-meter depths exhibited a rough surface profile. This was attributed to incomplete metal deposition caused by insufficient melting and transfer of the electrode material into the weld pool under underwater conditions. This was attributed to incomplete melting of the electrode, resulting in insufficient filler metal deposition within the weld joint. Therefore, in practical applications, a double-pass welding technique is required to ensure complete coverage and proper fusion of the weld seam. Nevertheless, examinations revealed that welds created with UW-1 electrodes at a depth of three meters exhibited seamless and comprehensive bead profiles, suggesting a thorough fusion and incorporation of the electrode metal [17]. At a depth of five meters, the surfaces of the weld bead were seen to exhibit incomplete fusion edges. This was caused by the hydrostatic pressure impacting the dispersion of the electrode metal prior to solidification.
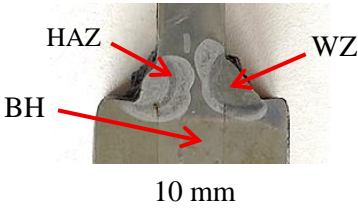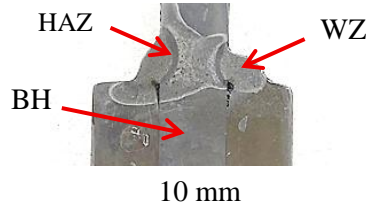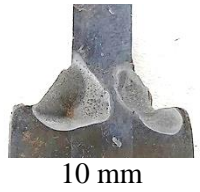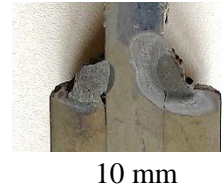
Table 2 Presents the examination of the weld surface through visual inspection.

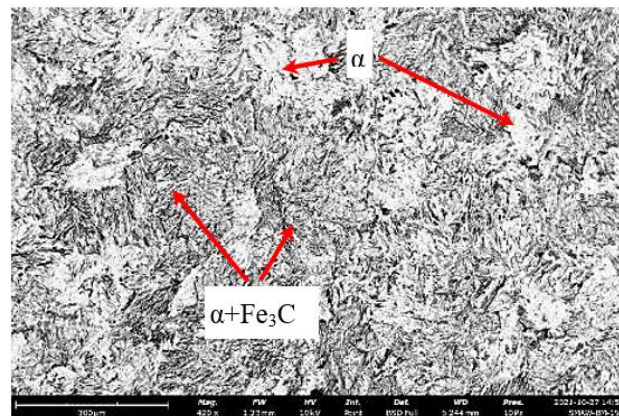| Variable	Weld Surface (mm)	
	3-meter depth	5-meter depth
E6013	30 mm	30 mm
UW-1	30 mm	30 mm

3.2 Results from the Macroscopic Structural Inspection

Table 3 presents the results of a macroscopic examination at 5× magnification using a macro lens. The welds produced by underwater welding exhibited similar macroscopic characteristics to those of air welding [12,13]. No cracks or porosity were observed in the weld zone (WZ) or the heat-affected zone (HAZ) for both E6013 and UW-1 electrodes. The weld joints displayed good fusion, which can be attributed to the application of the forehand welding technique and the optimized electrode angle, resulting in consistent metal transfer and improved visibility of the molten pool boundary. However, at a depth of five meters, incomplete penetration was observed. A distinct separation line between the joined plates was clearly visible, indicating insufficient fusion at this depth.

Table 3 Presents the macrostructure of underwater welding.

Variable	Macrostructure of underwater welding (mm)	
	3-meter depth	5-meter depth
E6013	10 mm	10 mm
UW-1	10 mm	10 mm

3.3 Results from the Microscopic Structure Examination

The microstructure of carbon steel grade AH36 (as shown in Figure 4), was examined using a SEM operated at an accelerating voltage of 10 kV. The observation was conducted on the base metal (BM) region. The results revealed that the primary microstructure consisted of pearlite, which is composed of two main phases: cementite (Fe_3C), appearing as the dark regions, and ferrite (α), appearing as the bright regions. The pearlitic structure was observed as alternating dark and light bands distributed uniformly throughout the examined area. This pattern indicates a well-controlled hot rolling process. Such a microstructure is typical of AH36-grade carbon steel, offering a balance of strength and toughness, making it suitable for marine structural applications, such as hulls and ship frames. [17,18].
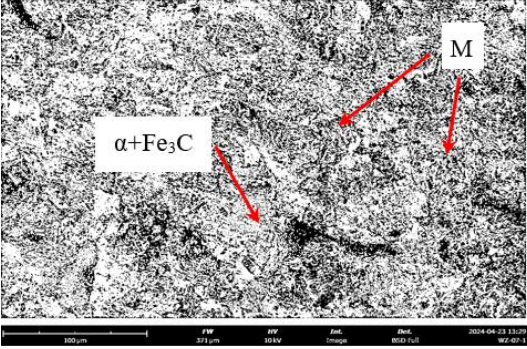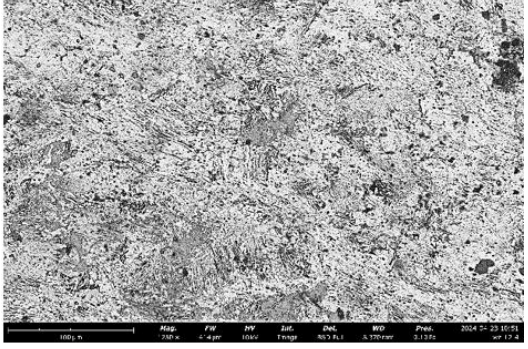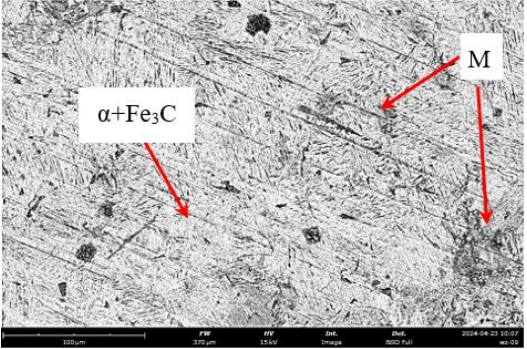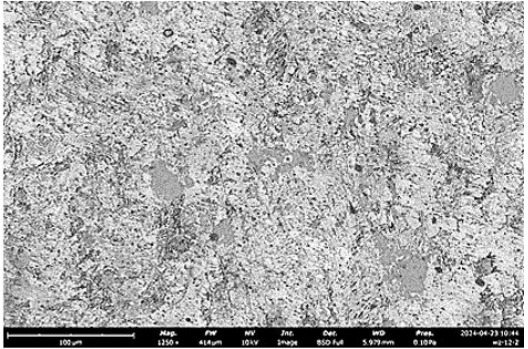

Figure 4 The microstructure of the base metal.

Based on the examination of the microstructure using scanning electron microscopy in the welded region (as indicated in Table 4), the structure is composed of alternating layers of martensite (M) and pearlite ($\alpha+Fe_3C$). Upon analyzing the metallographic structures of E6013 and UW-1 welding rods at depths of three and five meters, it was shown that E6013 welding results in a higher quantity of martensite in comparison to UW-1 welding. This is caused by the reduced viscosity of the E6013 flux, which leads to fast cooling properties.

Table 4 Presents the microstructure analysis of the weld zone using scanning electron microscopy.

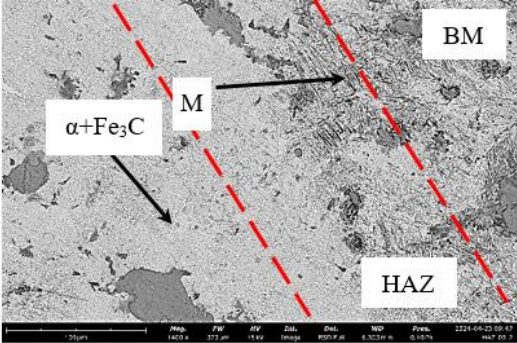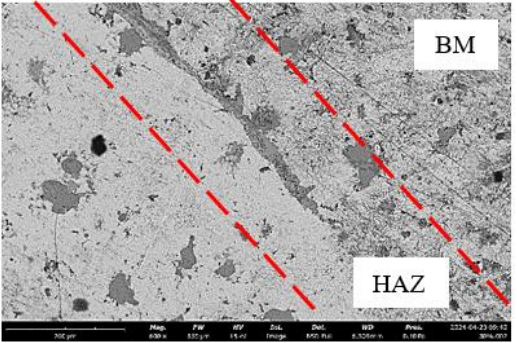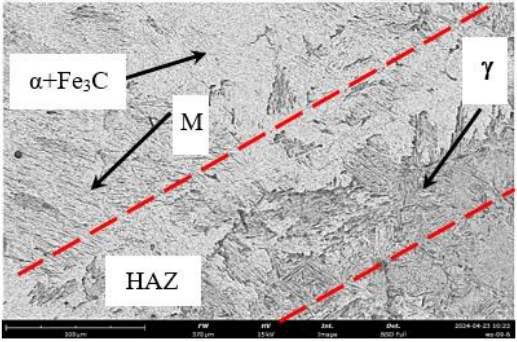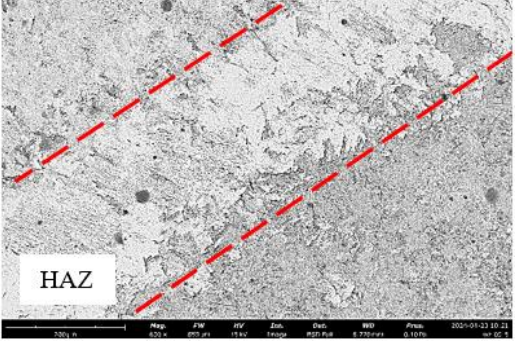| Variable	Microstructure of underwater welding (micron)	
	3-meter depth	5-meter depth
E6013		
UW-1		

The weld at a depth of three meters has a uniform arrangement of martensite interspersed with dispersed pearlite, which is more evenly distributed compared to the weld at a depth of five meters. The cooling rates and compression pressures during welding are influenced by the water pressure at depth [17,19]. However, after careful examination, it was determined that welding at a depth of three meters using UW-1 offers the most ideal distribution of the structure.

The examination of the microstructure in the HAZ using scanning electron microscopy revealed that welding with E6013 electrodes produces a microstructure that alternates between coarser martensite and pearlite, as indicated in Table 5. This is in contrast to welding with UW-1 electrodes [20,21,22]. Additionally, there is an imbalanced distribution of the structure and distinct demarcation layers between the HAZ and the base metal, which might result in cracking during operation.

The weld at a depth of three meters, displays a more evenly dispersed structure in comparison to the weld at five meters. This is due to the influence of water pressure, which affects cooling rates and compression throughout the welding process. The structure exhibits the distinctive characteristics of an austenitic structure (γ). Upon examination, it was discovered that welding at a depth of three meters using UW-1 produces an austenitic structure with a more even distribution [21,23].

Table 5 Presents the microstructure analysis of the heat-affected zone (HAZ) using scanning electron microscopy.

Variable	Microstructure of underwater welding (micron)	
	3-meter depth	5-meter depth
E6013		
UW-1		

Table 6 Analyzing the elemental composition using Energy Dispersive X-ray Spectroscopy technology at the weld zone of E6013 electrode at a depth of three meters (optimal).
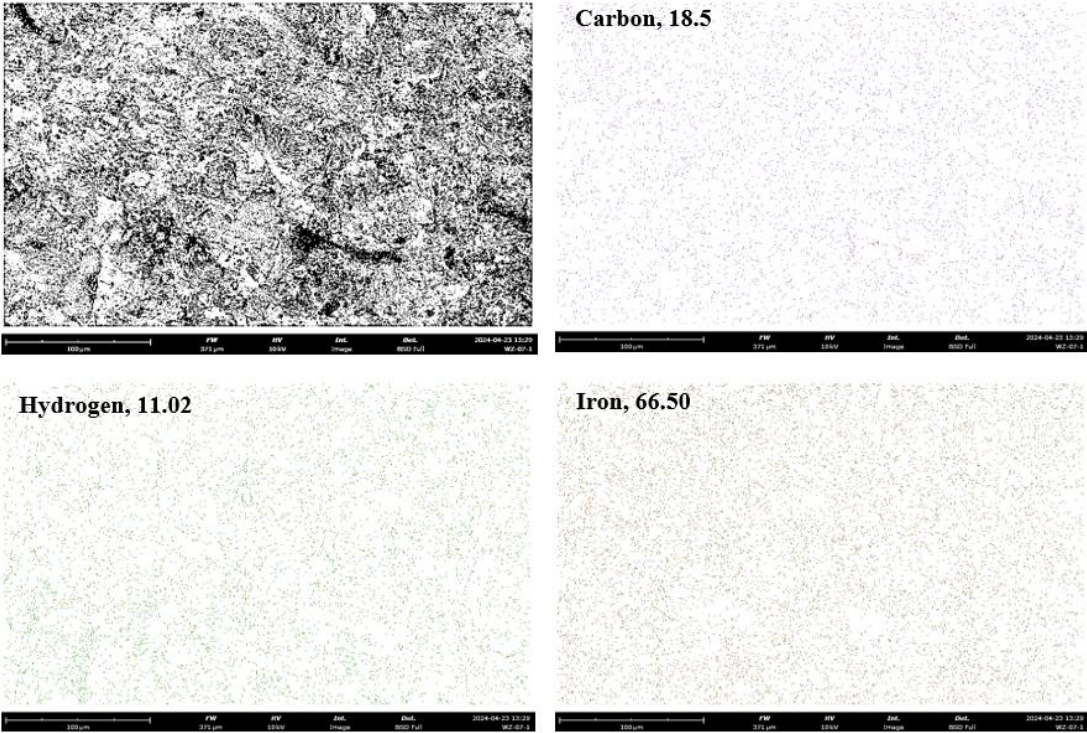
Table 6 provides an analysis of the WZ using Energy Dispersive X-ray Spectroscopy of E6013 electrodes at a depth of three meters (which is considered optimal). The examination revealed that the white areas consist of evenly distributed base metal, while the black areas contain carbon that is clustered together. Additionally, hydrogen is evenly distributed throughout the WZ.

Table 7 shows that, while utilizing Energy Dispersive X-ray Spectroscopy technology to examine the WZ at a depth of three meters, it was found that the white patches consist of equally scattered base metal. The regions that seem dark gray consist of hydrogen, which is distributed in clustered formations. The black regions are composed of equally dispersed carbon.

However, based on a review of existing data, it was found that the hydrogen content per unit area in underwater welds using the UW-1 electrode ranged between 7.0% and 11.7% of the area [23]. From the analysis presented in Tables 6 and 7, which compare the metallurgical structures of welds produced using E6013 and UW-1 electrodes at a depth of three meters, it was observed that welding with the E6013 electrode resulted in a hydrogen content of approximately 11.02% per area. This value is significantly higher than that of the UW-1 electrode, which showed a hydrogen content of approximately 6.50% per area. The higher hydrogen content in welds produced using the E6013 electrode is attributed to its flux composition, which is not well suited for underwater welding and tends to allow more water-derived hydrogen to enter the WZ [17,24,25]. In contrast, welds produced using the UW-1 electrode exhibited a more uniform elemental distribution and a lower hydrogen concentration in the WZ. This suggests that the use of proper electrode angle and the forehand welding technique can effectively reduce hydrogen absorption in underwater welds.

Table 7 Analyzing the elemental composition using Energy Dispersive X-ray Spectroscopy technology at the weld zone of UW-1 electrode at a depth of three meters (optimal).
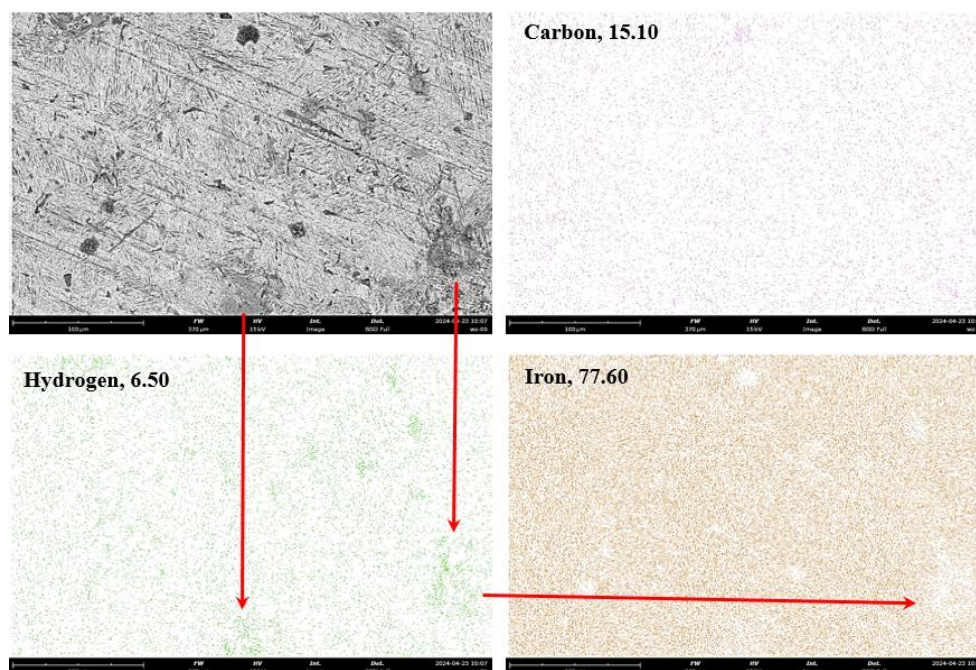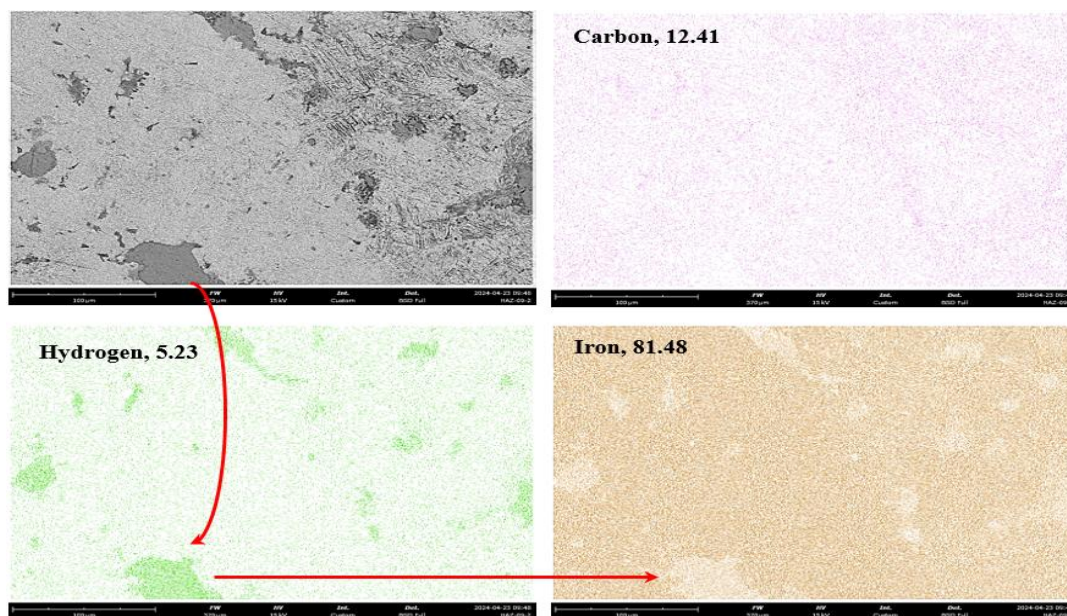

Table 8 reveals that Energy Dispersive X-ray Spectroscopy technology was employed to analyze the microstructure affected by the heat of E6013 welding wire at a depth of three meters. The analysis determined that the white regions primarily consist of the original metal, or iron, with widespread dispersion. The dark gray regions comprise distributed clusters of hydrogen (H). The black regions are composed of carbon and have a consistent and punctate arrangement.

Table 9 reveals that Energy Dispersive X-ray Spectroscopy technology was employed to analyze the microstructure affected by the heat of UW-1 welding wire at a depth of three meters, which is considered the ideal depth. The analysis determined that the white regions consist of original metal or iron with a consistent distribution. The dark gray regions comprise sparsely dispersed groups of hydrogen. Carbon is also present and evenly distributed.
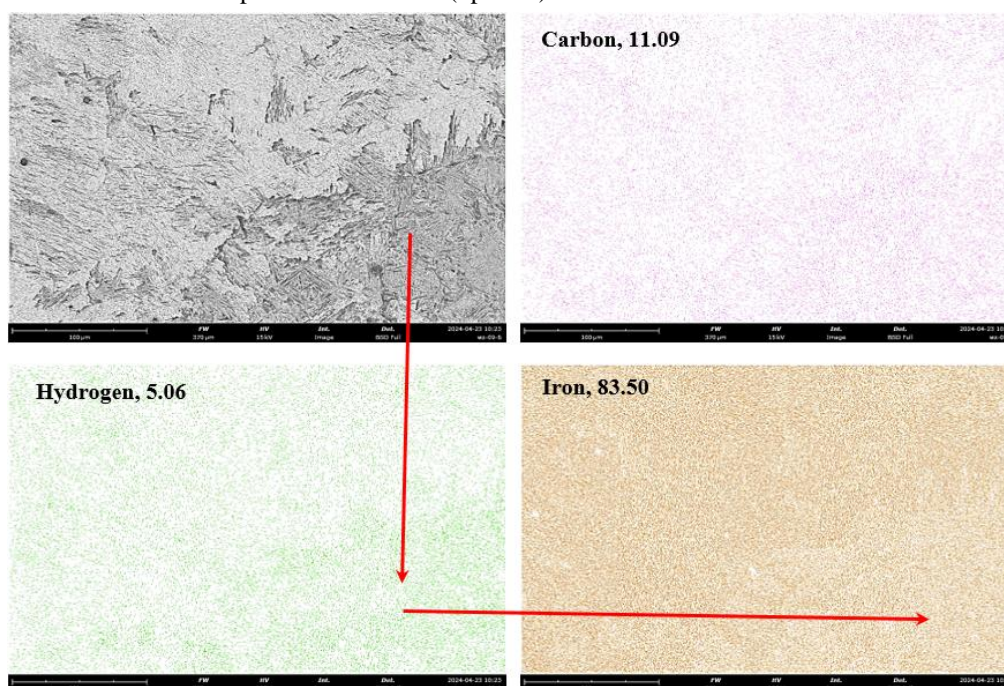
Table 8 Analyzing the elemental composition using Energy Dispersive X-ray Spectroscopy technology at the HAZ of E6013 electrode at a depth of three meters (optimal).

However, based on the analysis of Tables 8 and 9, which compare the metallurgical structures of the E6013 and UW-1 welding electrodes at a depth of three meters the optimal depth selected for this investigation it was found that the welds produced using the E6013 electrode exhibited a hydrogen content of 5.23% by area. This value is slightly higher than that observed for the UW-1 electrode, which recorded a hydrogen content of 5.06% by area. This result suggests that adjusting the electrode angle improves the flux coverage over the weld pool [25,26], while the use of the forehand welding technique facilitates better visibility of the molten pool and more stable metal transfer, effectively reducing hydrogen entrapment in the weld zone [27].

Furthermore, it was observed that the HAZ exhibited a lower hydrogen content compared to the WZ. This can be attributed to the faster cooling rate in the HAZ, which limits hydrogen diffusion and entrapment during the solidification process [23,28].

Table 9 Analyzing the elemental composition using Energy Dispersive X-ray Spectroscopy technology at the HAZ of UW-1 electrode at a depth of three meters (optimal).

3.4 Cost Evaluation of Underwater Welding Using E6013 and UW-1 Electrodes

From Table 10, a comparative cost analysis was conducted to evaluate the economic feasibility of using E6013 and UW-1 electrodes in underwater welding. The welding was performed on 9 mm thick AH36 steel plates in a lap joint configuration at depths ranging from three to five meters. Welding current was set at 250 A (DCEN polarity) using a 600 A-capacity welding machine. The evaluation considered consumable costs, power consumption, labor costs, and potential repairs due to welding defects.

Table 10 Summarizes the estimated welding cost per meter using both electrodes under identical underwater conditions.

Cost Component	E6013 (USD/meter)	UW-1 (USD/meter)
Electrode (1 kg)	2.72	28.78
Power Consumption	0.90	0.90
Labor Costs	53.03	53.03
Repairs Due to Defects	3.03	0.60
Total Estimated Costs	59.69	83.33

Although UW-1 exhibits higher initial electrode costs, it provides superior arc stability, lower hydrogen pickup, and a reduced risk of porosity and cracking in wet welding environments. These attributes contribute to a lower overall defect rate, minimizing the need for rework and post-weld inspection [29,30].

Conversely, the E6013 electrode, while cost-effective per unit, tends to experience unstable arc behavior underwater due to its conventional coating design. This often leads to increased weld discontinuities and additional repair work, thereby raising the total operational costs [31]. In conclusion, when structural reliability and long-term cost efficiency are priorities, especially in underwater applications, the UW-1 electrode is the more economically and technically viable choice despite its higher initial cost.

4. Conclusion

The weld bead surfaces produced using both E6013 and UW-1 electrodes met standard quality requirements. No porosity, slag inclusion, or cracks were observed. Notably, welding with UW-1 at a depth of three meters resulted in a smooth and uniform surface with complete fusion. This outcome is attributed to the use of the forehand welding technique and appropriate electrode angle control, which ensured stable metal transfer and clear visibility of the molten pool.

SEM microstructural analysis of the weld region revealed alternating M and pearlite (P) structures. The E6013 electrode produced a higher amount of martensite than the UW-1 electrode. In the HAZ, coarse pearlite and unevenly distributed martensite were observed, along with a clearly defined boundary between the HAZ and the base metal (BM).

EDS analysis of the weld area showed that the hydrogen content for E6013 was 11.02% by area, whereas UW-1 exhibited only 6.50%, which is below the typical hydrogen range in conventional underwater welding (7.0–11.7%). These results indicate the effectiveness of the forehand technique and proper electrode angle in reducing hydrogen accumulation. In the HAZ, the hydrogen content for E6013 was 5.23%, slightly higher than that of UW-1 at 5.06%.

Based on the experimental results, the E6013 electrode can be temporarily applied as a substitute for UW-1 in underwater welding applications. However, its use is recommended only for shallow depths not exceeding three meters, due to limitations in weld quality control at increased depths.

5. Acknowledgements

6. References

[1]   Klett J, Hassel T. Effect of water depth on hydrogen content in SMAW wet welded joints. SN Appl Sci. 2020;2:1269.

[2]   Verma K, Kumar H. Underwater welding: recent trends and future scope. Int J Emerg Technol. 2012;3(2):115-120.

[3]   Sundarapandiyan C, Balamurugan A, Mohan M. A review on underwater welding process. Int J Innov Eng Technol. 2017;8(1):260-265.

[4]   Liu L, Wang W, Wang S, Liu J, Feng J. Study on hydrogen-induced cracking in underwater wet welding. J Mater Process Technol. 2015;221:132-139.

[5]   Szczucka-Lasota B, Rogalski G, Szymczak C. Characteristics of wet welding with regard to the formation of defects. Arch Metall Mater. 2011;56(3):721-728.

[6]   Golikov N, Rogalski G. Effect of environmental conditions on diffusible hydrogen content during underwater wet welding. Weld Int. 2016;30(6):446-452.

[7]   Yousefi M, Ghaini FM. Influence of electrode angle and welding polarity on the quality of underwater welds. J Manuf Process. 2019;45:587-595.

[8]   Alajmi EF, Alqenaei AA. Underwater welding techniques. J Eng Res Appl. 2017;7(2):14-17.

[9]   Joshi MC, Rautela DS, Chauhan R, Suyal S. Scrutinize research on underwater welding process: a review. J Mech Civ Eng. 2016;13(5):74-78.

[10]   American Welding Society. Specification for carbon steel electrodes for shielded metal arc welding. 14th Edition. Miami (FL): AWS A5.1/A5.1M. 2012.

[11]   Kobayashi Y, Suga Y. Study on performance of new underwater welding electrode UW-1. Q J Jpn Weld Soc. 2011;29(1):63-67.

[12]   Dutta Majumdar J. Underwater welding: present status and future scope. J Naval Archit Mar Eng. 2014;3:39-48.

[13]   Ersoy E. Recent trends and development of underwater welding. Int J Eng Sci Appl. 2020;4(1):36-44.

[14]   Yousef MM, Mohamed MM, Abou-Bakr MH. Estimation of heat input and weld bead characteristics in SMAW. J Mater Process Technol. 2015;222:174-182.

[15]   Kim J, Lee S, Kim Y. Heat loss characteristics in underwater welding environments. J Mar Eng Technol. 2019;18(4):203-210.

[16]   Nakacho K, Matsumoto T, Tamura Y. Development of advanced electrodes for wet welding and its thermal behavior. Weld Int. 2021;35(12):935-943.

[17]   Wang J. Characterization of the underwater welding arc bubble through a visual sensing method. J Mater Process Technol. 2018;251:95-108.

[18]   Hikmatullah C. Environment effect on underwater wet welding process of API 5L X65 steel by coating resin-based E6013 electrode. J Trans Syst Eng. 2023;1(1):31-39.

[19]   Çolak Z, Ayan Y, Kahraman N. Weld morphology and mechanical performance of marine structural steel welded underwater in a real marine environment. Int J Adv Manuf Technol. 2020;109:491-501.

[20]   Vashishtha P. Problems encountered in underwater welding and remedies: a review. Innov Technol Mech Eng. 2022;64(3):1433-1439.

[21]   Li H. Microstructure and mechanical properties of underwater wet welded high-carbon-equivalent steel Q460 using austenitic consumables. J Mater Process Technol. 2017;249:149-157.

[22]   Klett J, Hassel T. Reducing the risk of hydrogen-induced cold cracks in hyperbaric wet welding of high-strength steels by using austenitic welding consumables. Int J Hydrogen Energy. 2020;45(19):54-60.

[23]   Tomków J, Fydrych D, Łabanowski J, Rogalski G. Effect of water depth on the structure and hardness of wet welded joints. Arch Civ Mech Eng. 2019;19(4):1233-1243.

[24]   Dariusz F, Rogalski G. Effect of shielded-electrode wet welding conditions on diffusion hydrogen content in deposited metal. Weld Int. 2011;25(3):166-171.

[25]   Sezgin B. Hydrogen energy systems for underwater applications. Int J Hydrogen Energy. 2022;47(45):19780-19796.

[26]   Nakpradit T, Poopat B. Investigation of diffusible hydrogen content and microstructure examination of underwater welding. Asia Pac J Sci Technol. 2010;3(3):45-51.

[27]   Santos VR. Prediction of hydrogen cracking in the wet welding of structural steels with ferritic stick electrodes down to 20 m. J Mater Res Technol. 2021;15:5787-5802.

[28]   Basha S, Reddy GM. Effect of welding technique on weld bead characteristics and hydrogen diffusion in wet welding. J Manuf Process. 2014;16(1):113-121.

[29]   Kovac M, Krajnik P, Dolšak B. Cost-benefit analysis of welding processes in offshore applications. J Manuf Sci Eng. 2020;142(5):051011.

[30]   Shamsudin M, Mohd A, Sulaiman S. Performance of underwater welding electrodes under varying depth conditions. Int J Offshore Polar Eng. 2019;29(2):114-121.

[31]   Kumar A, Dwivedi DK. Effect of moisture content in welding electrodes on the mechanical properties of weld metal. Mater Des. 2014;54:702-709.